

# **Design and Analysis of Partitioned-Stator Flux-Switching Hybrid-Excitation Machine for Hybrid Electric Vehicles**

Christopher H. T. Lee<sup>1</sup>, K. T. Chau<sup>2</sup>, C. C. Chan<sup>2</sup>, and T. W. Ching<sup>3</sup>

<sup>1</sup>*Research Laboratory of Electronics, Massachusetts of Technology, Cambridge, MA 02139, USA*

<sup>2</sup>*C. C. Chan (corresponding author), Department of Electrical and Electronic Engineering, The University of Hong Kong, Hong Kong, China, ccchan@eee.hku.hk*

<sup>3</sup>*Department of Electromechanical Engineering, University of Macau, Macao, China*

---

## **Summary**

In this paper, an advanced partitioned-stator flux-switching hybrid-excitation (PS-FSHE) machine, which is highly suitable for the hybrid electric vehicle (HEV), is proposed. By artfully implementing the two excitation sources, namely the high-energy-density permanent-magnet (PM) source and the DC-field excitation source, the hybrid machine can take the benefits from both sides. Unlike the existing PS-FSHE machines that sacrifice the PM materials for DC-field winding accommodation, the proposed machine instead shares the space of the armature winding with the DC-field winding. Hence, comparable power and torque densities can be potentially achieved. To verify the proposed concept and illustrate the merits of the proposed machine, the key machine performances are analysed and compared based on the finite element method (FEM).

*Keywords: flux-switching, hybrid electric vehicle, hybrid-excitation, partitioned-stator.*

---

## **1 Introduction**

Owing to the enhancing concerns on energy efficiency and environmental protection, the development of the hybrid electric vehicles (HEVs) has been accelerating [1] –[4]. Serving as the key component of the HEV systems, the electric machines are expected to fulfil several criteria [5]–[8]

- high efficiency
- high power and torque densities
- high controllability
- wide operating range
- maintenance-free

The flux-switching permanent-magnet (FSPM) machine can fulfil most of the requirements and this type of machine has attracted substantial attentions in the past years [9] –[11]. The partitioned-stator FSPM (PS-FSPM) machine, which can utilize the inner space to improve the machine performances, has been proposed recently [12]. Nevertheless, same as the other PM machines, the PS-FSPM machine also suffers from the undesirable flux-weakening performance.

To provide a better flux-weakening capability, the concept of the external flux adjuster (FA) has been developed [13] –[15]. With the installation of the mechanical FAs, the PM flux density can be short-circuited and weakened to a desirable level. However, the implemental of the mechanical FA arrangement suffers from the complicated structure. To improve the situation and to maintain the simplicity of the machine structure, the development of the hybrid-excitation (HE) machines have been regarded as a promising solution [16], [17]. However, the existing HE machine sacrifices the PM space for DC-field accommodation, such that the power density is highly deteriorated. Yet, the research on the HE machine with other topologies is still limited.

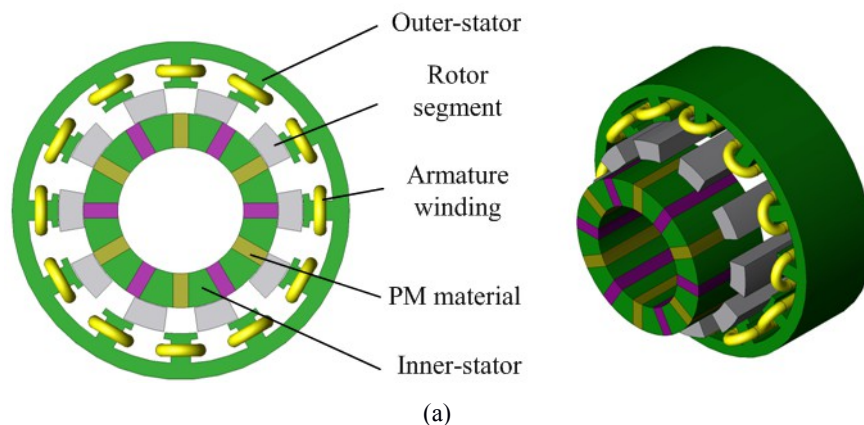
The purpose of this paper is to propose a new type of PS-FSHE machine for the HEV applications. Unlike the existing PS-FSHE machine that sacrifices the high-energy-density PM materials for DC-field winding accommodations, the proposed machine instead shares the space of the armature winding with the DC-field winding. Hence, comparable power and torque densities can be potentially achieved. To show the attractiveness of the proposed design, the PS-FSPM machine, the FA-PS-FSPM machine and the renowned Toyota Prius HEV machine will also be included for comprehensive analysis.

## 2 Partitioned-Stator Machines

The PS-FSPM machine, the FA-PS-FSPM machine and the PS-FSHE machine are shown in Figure 1. To have a fair comparison, all three machines employs the same topology, i.e., 3-phase 12/10-pole double-stator sandwiched-rotor topology. To avoid the magnetic saturation within a particular region, the armature windings and the PM materials are purposely installed in the outer-stator and the inner-stator separately. Since the three machines are the extension from the profound FSPM machine, their key design equations such as the pole arrangements can be derived from that of its ancestors [9]. The three proposed machines consist of the unique flux-weakening settlements, i.e., (i) the PS-FSPM machine can weaken its flux density based on the armature currents; (ii) the FA-PS-FSPM machine on the mechanical FA installation; and (iii) the PS-FSHE machine on the independent DC-field currents.

In the established arrangement, the PS-FSHE machine installs the DC-field windings in a way to share the spaces with the high-energy-density PM materials [15]. Consequently, the power and torque densities of the machine are lowered significantly. To improve the situation, the proposed PS-FSHE machine instead allocates the DC-field excitations to share the space with the armature windings. As a result, the proposed machine can potentially maintain comparable power and torque levels as compared with the PS-FSPM one.

All the three machines, namely the PS-FSPM machine, the FA-PS-FSPM machine, and the PS-FSHE machine are developed based on the passenger HEV specifications [10]. To offer a more comprehensive comparison, the popular Prius HEV machine is also included. To fairly compare all these machines, their most important machine dimensions, namely the outside diameters, stack lengths, and airgap lengths are set equal. In addition, the pole arcs, pole heights, slot-fill factors, and current densities are also optimized such that the magnetic saturations can be minimized.



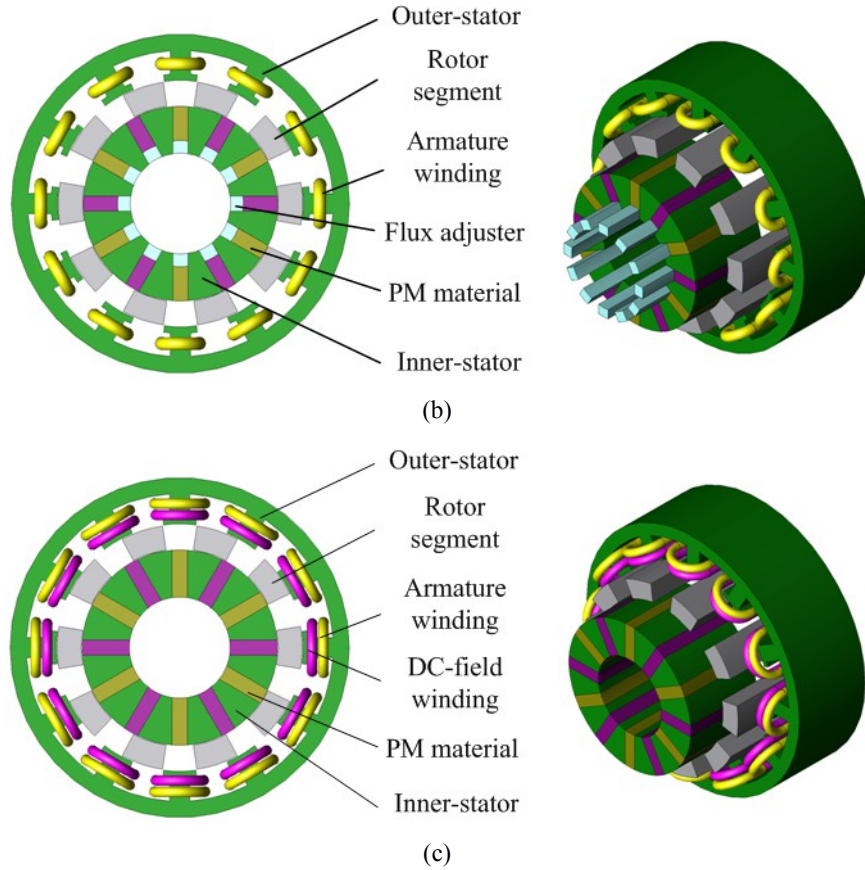


Fig. 1. Proposed machines: (a) PS-FSPM. (b) FA-PS-FSPM. (c) PS-FSHE.

### 3 Principle of Operations

To explain the operating principles of the bipolar flux-linkage characteristics of the proposed machines, the PM flux flows of the PS-FSPM machine are shown in Figure 2. It should be noted that all three proposed machines illustrate the same flux flow patterns, i.e., when the rotor segment moves from position 1 to 2, the flux flows switch its directions correspondingly. Consequently, the proposed machines can result the bipolar flux-linkage characteristics, and these machines can potentially generate higher power and torque densities than the unipolar counterparts do [7].

Because the three proposed machines are developed from the fundamental FSPM ancestors, these machines can also be operated with the profound bipolar conduction schemes [6]. In particular, the sinusoidal armature current  $I$  is injected according to the status of the bipolar flux-linkage  $\Psi$ . Consequently, the positive electromagnetic torque  $T$  can be produced. This conduction scheme is so-called as the brushless AC (BLAC) conduction scheme, as shown in Figure 3. With the employment of the BLAC conduction scheme, the proposed machines can seamlessly interact with the employed armature currents, and hence the undesirable torque pulsation can be minimized. The sinusoidal armature currents for the proposed machines can be described as

$$\begin{cases} i_a = I_{peak} \sin \theta \\ i_b = I_{peak} \sin(\theta - (2\pi/3)) \\ i_c = I_{peak} \sin(\theta + (2\pi/3)) \end{cases} \quad (1)$$

where  $i_a$ ,  $i_b$ ,  $i_c$  and  $I_{peak}$  are the corresponding armature currents and the peak value of the phase currents, respectively.

Aforementioned, the three proposed machines can weaken its PM flux densities with its distinguished approaches. In particular, the PS-FSPM machine can weaken its PM flux densities by the control of armature currents. Meanwhile, the FA-FSPM machine can utilize the mechanical FAs to short-circuit the PM flux flows, as shown in Figure 4(a). As a result, the FA-FSPM machine can provide outstanding flux-weakening capability. On the other hand, the hybrid PS-FSHE machine can independently control its DC-field currents to weaken the PM flux density, as shown in Figure 4(b). Consequently, the hybrid machine can offer both satisfactory PM flux density and reasonable flux-weakening capability simultaneously.

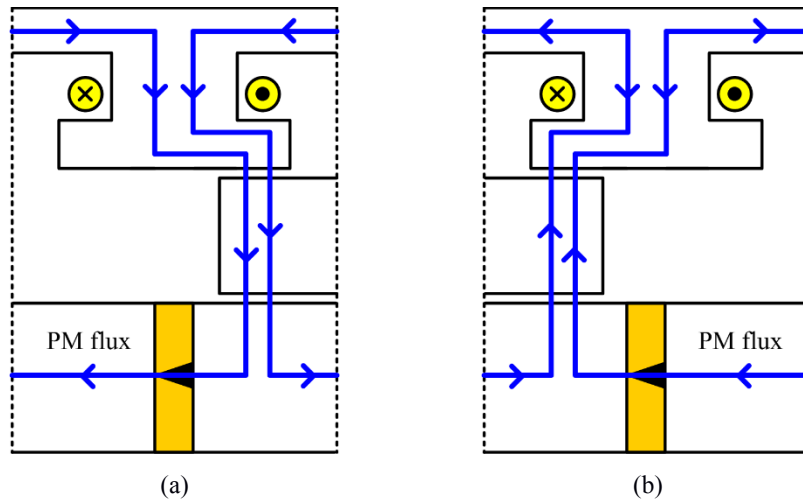


Figure 2: Flux flow patterns of PS-FSPM machine: (a) Position 1. (b) Position 2.

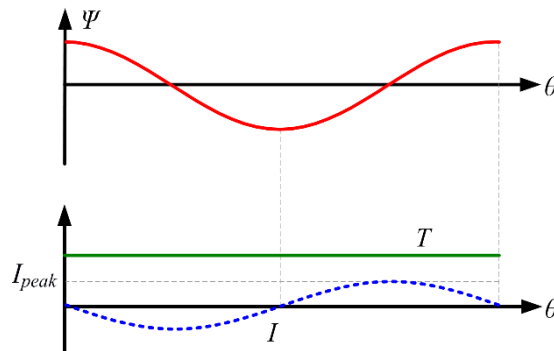


Figure 3: Brushless AC conduction scheme.

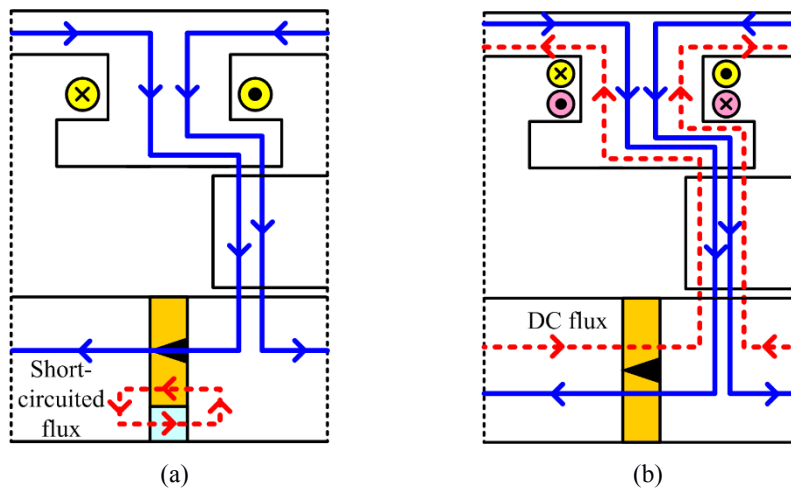


Figure 4: Flux-weakening principles: (a) FA-PS-FSPM. (b) PS-FSHE.

## 4 Electromagnetic Field Analysis

The electromagnetic field analysis has been generally accepted as the most convenient and accurate tools to analyse the electric machine performances [6]. In this paper, a well-defined commercial finite element method (FEM) software, the JMAG-Designer is employed to analyse the machine performances. With the iterative approaches, the optimization of the key machine parameters can be achieved. Consequently, all three proposed machines can be compared quantitatively with the fair environment. The Prius HEV machine is also included for illustration purposes, while the key design data is listed in Table I.

The aims of this paper are to offer the design criteria and quantitative comparisons of the three proposed machines, such that the use of simulation results is more preferable. Upon the support of the FEM results, the unexpected errors of the manufacture imperfection can be minimized. However, the experimental verifications are always indispensable. Hence, the proposed machines will be prototyped, while the experimental data will be included in our future papers.

TABLE I. KEY MACHINE DESIGN DATA [15]

Item	Prius	PS-FSPM	FA-PS-FSPM	PS-FSHE
Outer-stator outside diameter	269 mm	269 mm	269 mm	269 mm
Outer-stator inside diameter	161.86 mm	194.86 mm	194.86 mm	194.86 mm
Rotor outside diameter	160.4 mm	193.4 mm	193.4 mm	193.4 mm
Rotor inside diameter	110.64 mm	155.86 mm	155.86 mm	155.86 mm
Inner-stator outside diameter	N/A	154.4 mm	154.4 mm	154.4 mm
Inner-stator inside diameter	N/A	110.64 mm	80 mm	80 mm
Airgap length	0.73 mm	0.73 mm	0.73 mm	0.73 mm
Stack length	83.56 mm	83.56 mm	83.56 mm	83.56 mm
Number of stator slots	48	12	12	12
Number of rotor poles	8	10	10	10
Number of phases	3	3	3	3
Number of armature turns	13	33	33	18

## 5 Machine Performance Analysis

### 5.1 Machine performance at no-load conditions

The flux-linkage waveforms of the proposed machines are shown in Figure 5. Since all three machines consist of the same operating principles, their flux-linkage patterns are very similar. In particular, the three machines can all produce the bipolar flux-linkage characteristics. As shown, the PS-FSPM machine exhibits the greatest flux-linkage values, such that it can potentially produce the highest power and torque levels among the group.

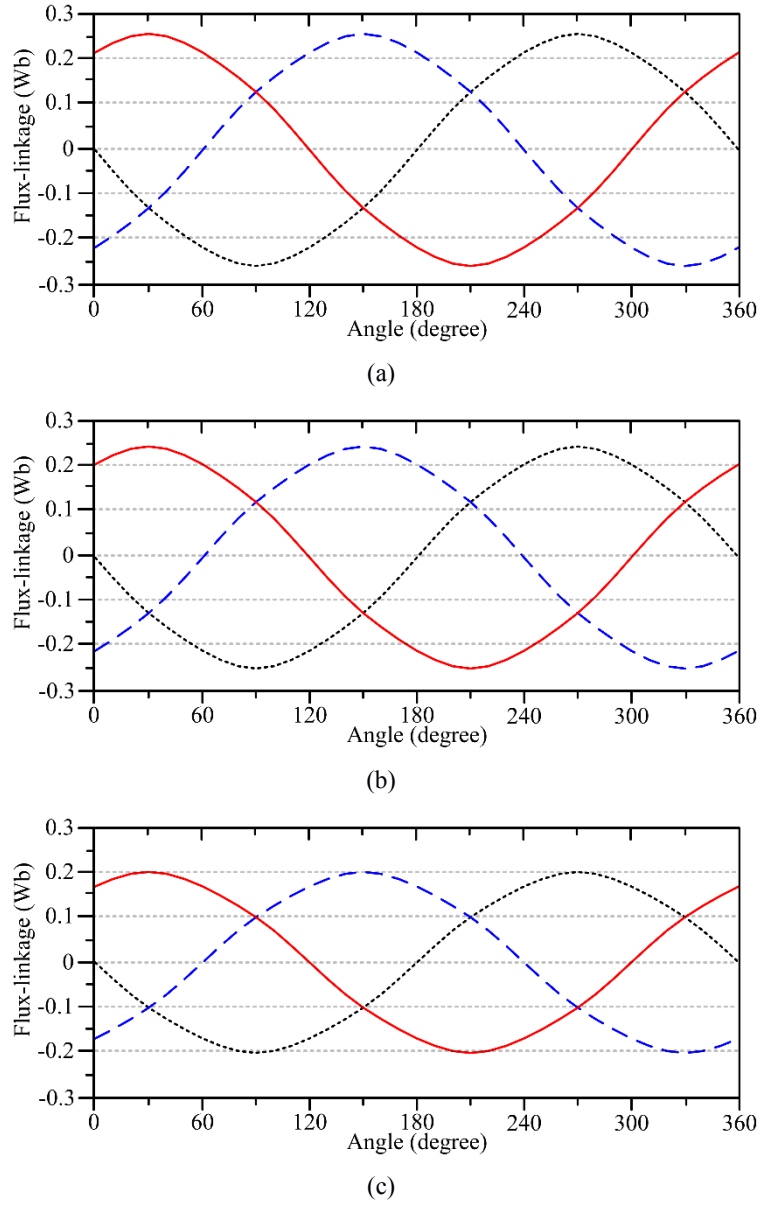


Figure 5: Flux-linkage waveforms: (a) PS-FSPM. (b) FA-PS-FSPM. (c) PS-FSHE.

## 5.2 Torque performance analysis

The output torque waveforms of the proposed machines at rated conditions are shown in Figure 6. It should be noted that the PS-FSPM machine can only utilize the armature excitations for flux-regulating operation, and its steady torque can reach up to 358 Nm. In the meantime, the FA-PS-FSPM machine under three situations, namely with no FAs, with alternative FAs, and with all FAs installations are around 342 Nm, 243 Nm, and 188 Nm, respectively. In addition, the PS-FSHE machine under three situations, namely with  $I_{DC} = 0 \text{ A/mm}^2$ ,  $I_{DC} = -15 \text{ A/mm}^2$ , and  $I_{DC} = -30 \text{ A/mm}^2$  are about 336 Nm, 308 Nm, and 287 Nm, respectively.

Moreover, the torque ripple percentage  $K_{ripple}$  can be calculated based on the following relationship

$$K_{ripple} = \frac{T_{max} - T_{min}}{T_{avg}} \times 100 \% \quad (2)$$

where  $T_{avg}$ ,  $T_{max}$ , and  $T_{min}$  are the average, maximum, and minimum torque values, respectively. It can be observed that the torque ripples of the PS-FSPM machine is about 6.7 %. The torque ripples of the FA-PS-

FSPM machine under corresponding situations are about 7.7 %, 11.2 %, and 15.1 %, while of the PS-FSHE machine are about 7.2 %, 10.4 %, and 13.5 %.

To offer a more comprehensive analysis of torque performances, the cogging torques of the proposed machines are shown in Figure 7. It can be found the cogging torques of the PS-FSPM machine is about 28.9 Nm, where it is around 8.1 % of its steady torques. For the FA-PS-FSPM machine, its cogging torques are 27.5 Nm, 13.8 Nm, and 7.9 Nm, as 8 %, 5.7 %, and 4.2 % of its steady torques. For the PS-FSHE machine, its cogging torques are 26.2 Nm, 15.7 Nm, and 11.7 Nm, as 7.8 %, 5.1 %, and 4.1 % of its steady torques.

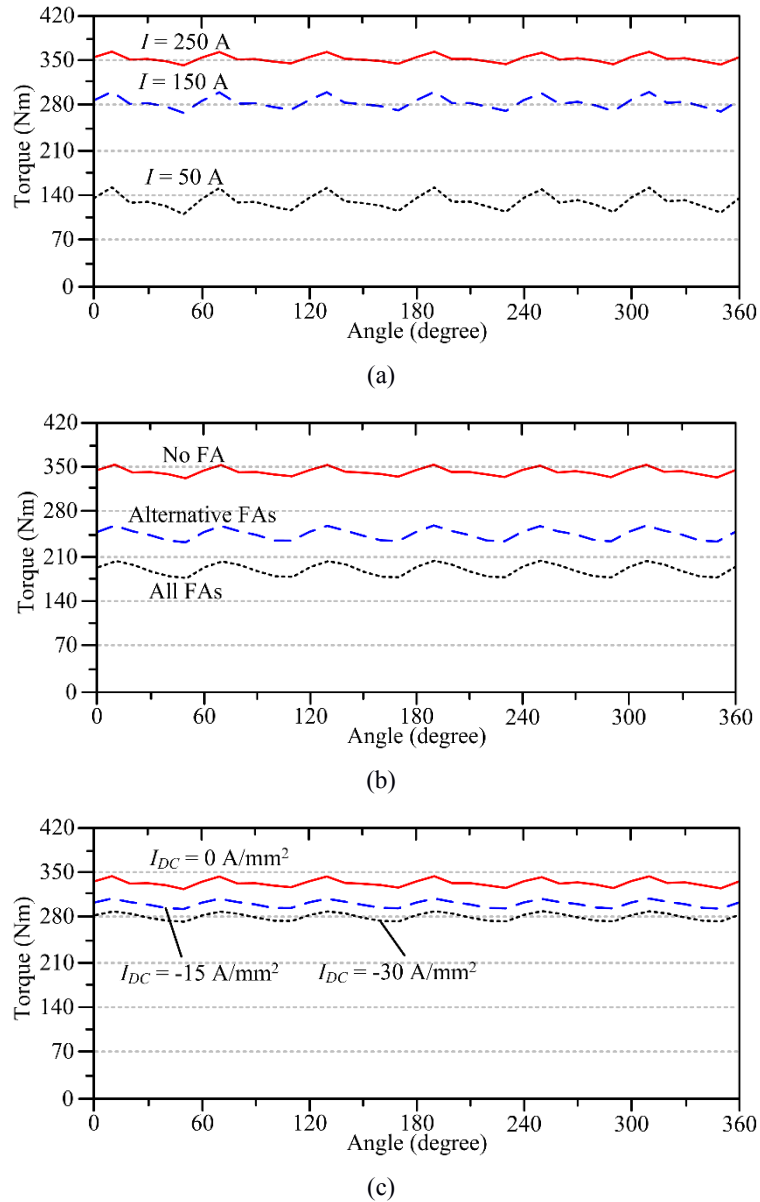


Figure 6: Output torque waveforms: (a) PS-FSPM. (b) FA-PS-FSPM. (c) PS-FSHE.

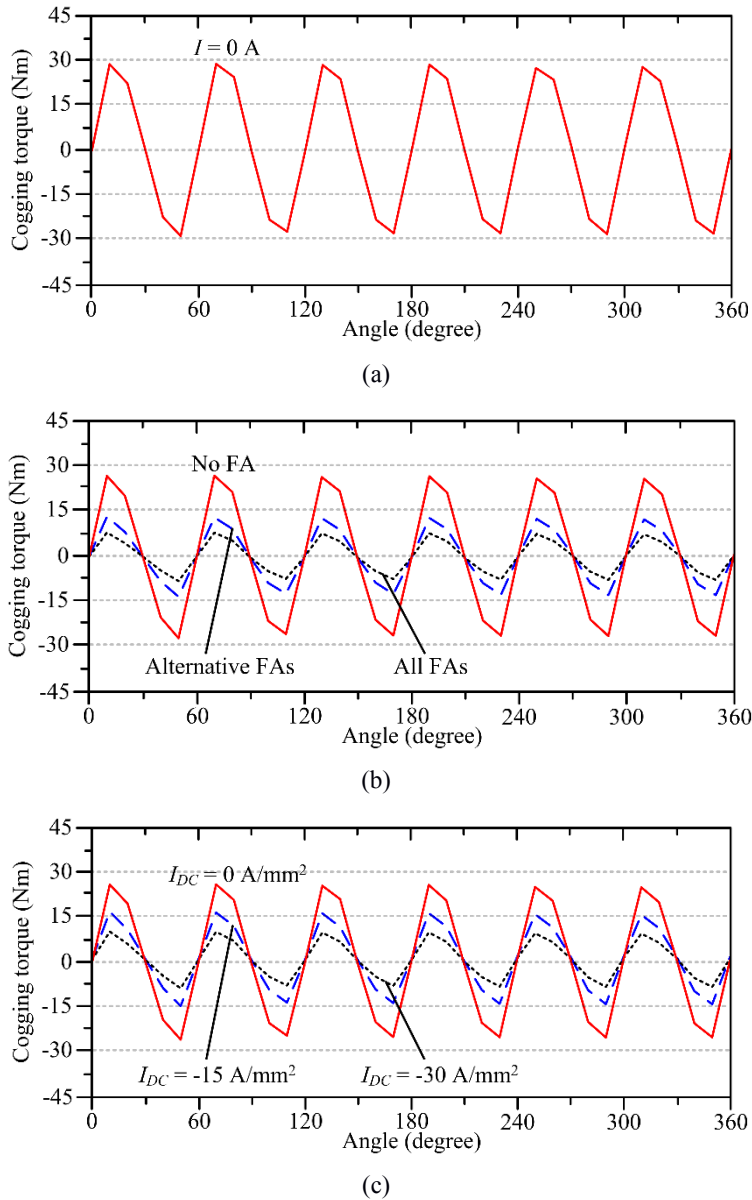


Figure 7: Cogging torque waveforms: (a) PS-FSPM. (b) FA-PS-FSPM. (c) PS-FSHE.

### 5.3 Flux-weakening performance analysis

The flux-weakening capability between the PS-FSHE and the FA-PS-FSPM machines are studied, while their no-load EMF waveforms with respect to various operating speeds are shown in Figure 8. With the employment of the external FAs, it can be shown that the FA-PS-FSPM machine can weaken its no-load EMF values for about 47 %. In the meantime, when the DC-field windings are excited negatively, i.e.,  $I_{DC} = -30 \text{ A/mm}^2$ , the PS-FSHE machine can only weaken its no-load EMF values for about 18 %. As a result, it can be shown that the proposed FA-PS-FSPM machine can provide better flux-weakening performance than the PS-FSHE machine does.

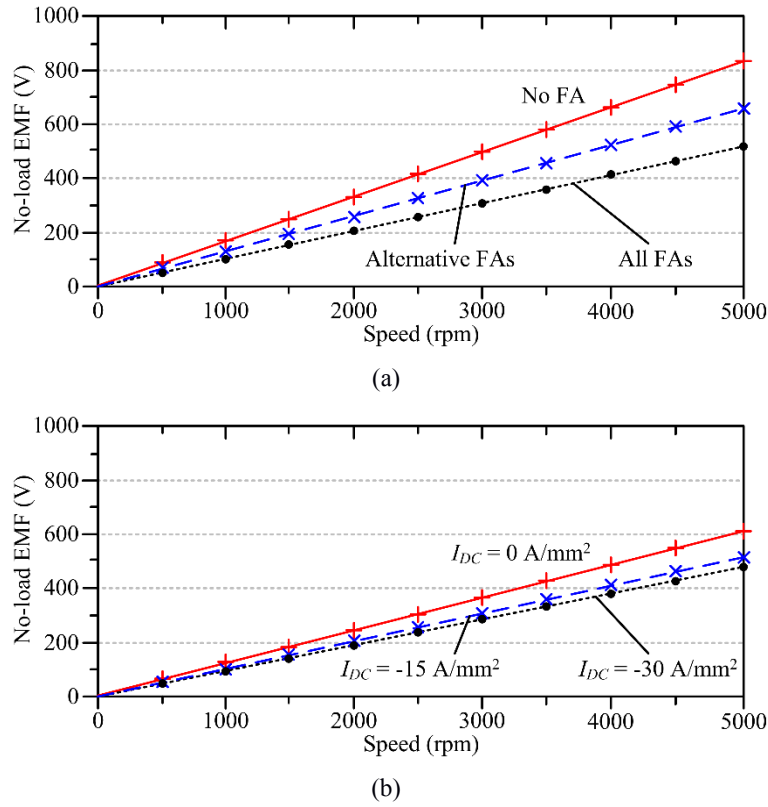


Figure 8: No-load EMFs at various speeds: (a) FA-PS-FSPM. (b) PS-FSHE.

TABLE II. MACHINE PERFORMANCE COMPARISONS [15]

Item	Prius	PS-FSPM	FA-PS-FSPM	PS-FSHE
Efficiency	86 %	87 %	87 %	87 %
Power	46200 W	45000 W	43000 W	42200 W
Base speed	1200 rpm	1200 rpm	1200 rpm	1200 rpm
Output torque	368 Nm	358 Nm	342 Nm	336 Nm
Torque ripple	20.7 %	6.7 %	7.7 %	7.2 %
Cogging torque	N/A	28.9 Nm	27.5 Nm	26.2 Nm
Total mass	32.9 kg	30.8 kg	31.2 kg	31.0 kg
Power density	1404 W/kg	1461 W/kg	1378 W/kg	1361 W/kg
Torque density	11.2 Nm/kg	11.6 Nm/kg	11.0 Nm/kg	10.8 Nm/kg
Material cost	US 95.4	US 116.2	US 117.3	US 121.2
Power / cost	484 W/US	387 W/US	367 W/US	348 W/US
Torque / cost	3.9 Nm/US	3.1 Nm/US	2.9 Nm/US	2.8 Nm/US

## 6 Machine Performance Evaluations

All the key performances of the proposed machines are summarized in Table II. To show the potentials and attractiveness of the proposed machines, the popular Prius HEV machine is also included for comparisons.

With the substantial installation of high-energy-density PM materials, the proposed PS-FSPM machine can provide the highest torque and power densities among the comparing group. As a result, this characteristic is very attractive for the high-end HEV users.

Nevertheless, the supply of PM materials is limited, such that the PM materials have become the dominating expenses for machine constructions [18]. Undoubtedly, the cost-effectiveness must be one of the most important factors that interferes the HEV market value, such that it should be considered carefully. In particular, the key material costs, namely the laminated iron, the PM material, and the copper, can be found based on the market price. It should be noted that the Prius machine can achieve the best cost-effectiveness among the peer group, and this is the reason why this machine type is so popular in the HEV market.

To offer a more representative evaluation for the proposed machines, a grading system is employed as shown in Table III. The grading system consists of six most important criteria and each of them is graded from score 1 to 5, where 1 means the worst and 5 the best. Consequently, when all the criteria are included, the hybrid PS-FSHE machine will become a very attractive candidate for the HEV applications.

TABLE III. EVALUATIONS ON THE PROPOSED MACHINES

Item	Prius	PS-FSPM	FA-PS-FSPM	PS-FSHE
Efficiency	3	4	4	4
Power and torque densities	4	5	4	4
Cost-effectiveness	5	4	3	3
Flux-weakening capability	1	2	5	4
Operating range	1	1	4	3
Mechanical integrity	5	4	1	4
<b>Total</b>	<b>19</b>	<b>20</b>	<b>21</b>	<b>22</b>

## 7 Conclusion

In this paper, three PS machines, namely the PS-FSPM machine, the FA-PS-FSPM machine, and the PS-FSHE machine have been analysed and compared based on the key criteria. With the employment of the two excitation sources, the PS-FSHE machine exhibits excellent performances in various aspects. In particular, the proposed PS-FSHE machine purposely maintains substantial PM material for excitation, such that it can provide adequate power and torque densities for the HEV applications. By including all the key criteria into the basket, the PS-FSHE machine has shown good potential for the HEV industry.

## Acknowledgments

This work was supported by Croucher Foundation, Hong Kong Special Administrative Region, China.

## References

- [1] K. T. Chau and C. C. Chan, "Emerging energy-efficient technologies for hybrid electric vehicles," *Proc. IEEE*, vol. 95, no. 4, pp. 821–835, Apr. 2007.
- [2] A. Emadi, Y. J. Lee, and K. Rajashekara, "Power electronics and motor drives in electric, hybrid electric, and plug-in hybrid electric vehicles," *IEEE Trans. Ind. Electron.*, vol. 55, no. 6, pp. 2237–2245, Jun. 2008.
- [3] A. Y. Saber, and G. K. Venayagamoorthy, "Plug-in vehicles and renewable energy sources for cost and emission reductions," *IEEE Trans. Ind. Electron.*, vol. 58, no. 4, pp. 1229–1238, Apr. 2011.
- [4] C. H. T. Lee, K. T. Chau, and C. Liu, "Design and analysis of an electronic-gearless magnetless machine for electric vehicles," *IEEE Transactions on Industrial Electronics*, vol. 63, no. 11, pp. 6705–6714, November 2016.
- [5] Z. Q. Zhu, and D. Howe, "Electrical machines and drives for electric, hybrid, and fuel cell vehicles," *Proc. IEEE*, vol. 95, no. 4, pp. 746–765, Apr. 2007.
- [6] K. T. Chau, C. C. Chan, and C. Liu, "Overview of permanent-magnet brushless drives for electric and hybrid electric vehicles," *IEEE Trans. Ind. Electron.*, vol. 55, no. 6, pp. 2246–2257, Jun. 2008.
- [7] M. Cheng, W. Hua, J. Zhang, and W. Zhao, "Overview of stator-permanent magnet brushless machines," *IEEE Trans. Ind. Electron.*, vol. 58, no. 11, pp. 5087–5101, Nov. 2011.
- [8] C. H. T. Lee, K. T. Chau, and L. B. Cao, "Development of reliable gearless motors for electric vehicles," *IEEE Trans. Magn.*, accepted.
- [9] J. T. Chen, and Z. Q. Zhu, "Winding configurations and optimal stator and rotor pole combination of flux-switching PM brushless AC machines," *IEEE Trans. Energy Convers.*, vol. 25, no. 2, pp. 293–302, Jun. 2010.
- [10] R. Cao, C. Mi, and M. Cheng, "Quantitative comparison of flux-switching permanent-magnet motors with interior permanent magnet motor for EV, HEV, and PHEV applications," *IEEE Trans. Magn.*, vol. 48, no. 8, pp. 2374–2384, Aug. 2012.
- [11] R. P. Deodhar, A. Pride, S. Iwasaki, and J. J. Bremner, "Performance improvement in flux-switching PM machines using flux diverters," *IEEE Trans. Ind. Appl.*, vol. 50, no. 2, pp. 937–978, Mar./Apr. 2014.
- [12] D. J. Evans, and Z. Q. Zhu, "Novel partitioned stator switched flux permanent magnet machines," *IEEE Trans. Magn.*, vol. 51, no. 1, p. 8100114, Jan. 2015.
- [13] Z. Q. Zhu, M. M. J. Al-Ani, X. Liu, and B. Lee, "A mechanical flux weakening method for switched flux permanent magnet machines," *IEEE Trans. Energy Convers.*, vol. 30, no. 2, pp. 806–815, Jun. 2015.
- [14] C. H. T. Lee, J. L. Kirtley, M. Angle, and H. Nian, "Quantitative comparison of partitioned-stator machines for hybrid electric vehicles," *CES Transactions on Electrical Machines and Systems*, vol. 1, no. 2, pp. 146–153, Jun. 2017.
- [15] C. H. T. Lee, J. L. Kirtley, and M. Angle, "A partitioned-stator flux-switching permanent-magnet machine with mechanical flux adjusters for hybrid electric vehicles," *IEEE Trans. Magn.*, accepted.
- [16] Y. Amara, L. Vido, M. Gabsi, E. Hoang, A. H. B. Ahmed, and M. Lecrivain, "Hybrid excitation synchronous machines: Energy-efficient solution for vehicles propulsion," *IEEE Trans. Veh. Technol.*, vol. 58, no. 5, pp. 2137–2149, Jun. 2009.
- [17] W. Hau, Xiaomei, Yin, G. Zhang, and M. Cheng, "Analysis of two novel five-phase hybrid-excitation flux-switching machines for electric vehicles," *IEEE Trans. Magn.*, vol. 50, no. 11, p. 8700305, Nov. 2014.
- [18] C. H. T. Lee, K. T. Chau, C. Liu, and C. C. Chan, "Overview of magnetless brushless machines," *IET Electr. Power Appl.*, accepted.

## Authors

Christopher H. T. Lee received the B.Eng. (first class honours) degree, and Ph.D. degree both in electrical engineering from Department of Electrical and Electronic Engineering, The University of Hong Kong, Hong Kong. During the Ph.D. study, he was co-supervised by Prof. C. C. Chan and Prof. K. T. Chau.

He currently serves as the Postdoctoral Fellow in Research Laboratory of Electronics, Massachusetts Institute of Technology, and also the Honorary Assistant Professor in the alma mater. His research interests include electric motors and drives, renewable energies, and electric vehicle technologies. He is the author and co-author of 3 book chapters, 2 patents, and 60 international referred papers.

Dr. Lee received many awards, including the Croucher Foundation Fellowship to support his postdoctoral research and the Li Ka Shing Prize (the best Ph.D. thesis award).

K. T. Chau received his B.Sc. (Eng.) degree with first class honours, M.Phil. degree, and Ph.D. degree from The University of Hong Kong, Hong Kong, all in electrical and electronic engineering.

He joined the alma mater in 1995, and currently serves as the Associate Dean in the Faculty of Engineering and the Professor in the Department of Electrical and Electronic Engineering. His main research interests include electric vehicle technologies, renewable energy systems, and machines and drives. In these areas, he has published 7 books, 9 book chapters, and more than 250 refereed journal papers.

Prof. Chau is the Fellow of the HKIE, the IEEE, and the IET. He has served as Chairs and Organizing Committee Member for many international conferences. He has received many awards, including the Chang Jiang Chair Professorship, the Environmental Excellence in Transportation Award for Education, Training and Public Awareness, and the Award for Innovative Excellence in Teaching, Learning and Technology.

C. C. Chan received the B.Sc., M.Sc., and Ph.D. degrees in electrical engineering from China University of Mining & Technology, Tsinghua University and The University of Hong Kong, in 1957, 1959, and 1982, respectively.

He is currently the Honorary Professor and the former Head of the Department of Electrical and Electronic Engineering, The University of Hong Kong, Pokfulam, Hong Kong. He has had more than ten years industrial experience and more than 35 years academic experience.

Prof. Chan is the President of the HKIE in 1999/2000, the Founding President of the International Academy for Advanced Study, China, the Cofounder and Rotating President of the World Electric Vehicle Association, and the President of the Electric Vehicles Association of Asia Pacific. He is the Honorary Fellow of the HKIE, Fellow of the IEEE, the IET, the Royal Academy of Engineering, U.K., the Chinese Academy of Engineering, and The Ukraine Academy of Engineering Sciences. His major honours include the awards of Hong Kong Institution Gold Medal in 2010, World Federation of Engineering Organizations (WFEO) Medal of Engineering Excellence in 2013, the Royal Academy of Engineering Prince Phillip.

T. W. Ching received the B.Eng. and M.Sc. degrees in Electrical Engineering from The Hong Kong Polytechnic and the Ph.D. degree in Electrical and Electronic Engineering from The University of Hong Kong, in 1993, 1995, and 2002, respectively.

Dr. Ching served 11 years in industry with CLP Power Ltd., Hong Kong. He is currently an Assistant Professor of the University of Macau. His research interests include clean energy and environment, engineering economics, power electronic converters, variable speed drives, electric vehicles and charging infrastructure.